detectCilia: An R Package for Automated Detection and Length Measurement of Primary Cilia

Kai Budde-Sagert[1,2], Simone Krueger[3,4], Clemens Sehlke[3], Heiko Lemcke[4,5], Anika Jonitz-Heincke[3], Robert David[4,5], Rainer Bader[3,4] and Adelinde M Uhrmacher[2,4]

[1]Institute of Communications Engineering, University of Rostock, Rostock, Germany. [2]Institute for Visual and Analytic Computing, University of Rostock, Rostock, Germany. [3]Research Laboratory for Biomechanics and Implant Technology, Department of Orthopedics, Rostock University Medical Center, Rostock, Germany. [4]Department of Life, Light, and Matter, Interdisciplinary Faculty, University of Rostock, Rostock, Germany. [5]Reference and Translation Center for Cardiac Stem Cell Therapy, Department of Cardiac Surgery, Rostock University Medical Center, Rostock, Germany.

ABSTRACT

BACKGROUND AND OBJECTIVE: The primary cilium is a small protrusion found on most mammalian cells. It acts as a cellular antenna, being involved in various cell signaling pathways. The length of the primary cilium affects its function. To study the impact of physical or chemical stimuli on cilia, their lengths must be determined easily and reproducibly.

METHODS: We have developed and evaluated an open-source R package called detectCilia to detect and measure primary cilia automatically. As a case study to demonstrate the capability of our tool, we compared the influence of 4 different cell culture media compositions on the lengths of primary cilia in human chondrocytes. These media compositions include (1) insulin-transferrin-selenium (ITS); (2) ITS and dexamethasone (Dexa); (3) ITS, Dexa, insulin-like growth factor 1 (IGF-1), and transforming growth factor beta 1 (TGF-β1); and (4) fetal bovine serum (FBS).

RESULTS: The assessment of detectCilia included a comparison with 2 similar tools: ACDC (Automated Cilia Detection in Cells) and CiliaQ. Several differences and advantages of our package make it a valuable addition to these tools. In the case study, we have observed variations in the ciliary lengths associated with using different media compositions.

CONCLUSIONS: We conclude that detectCilia can automatically and reproducibly detect and measure primary cilia in confocal microscopy images with low false-positive rates without requiring extensive user interaction.

KEYWORDS: Primary cilium, automated image analysis, R package, reproducibility, confocal microscopy

Introduction

The primary cilium is a specialized structure that extends from the cell surface like a solitary hair. In contrast to motile cilia of epithelial cells, primary cilia do not have a central pair of single microtubules, which makes them immotile. This single microtubule-based structure is present in most mammalian cell types found in connective tissues (eg, chondrocytes), epidermis, reproductive organs, and stem cells.[1,2] For a long time, the primary cilium was considered a rudimentary structure without any function in multicellular organisms.[3]

Since the early 2000s, the primary cilium has gained more attention in research as it is involved in various signaling pathways and homeostasis, and can be associated with cancer development.[4] The importance of the primary cilium is also evident when abnormalities are present, which may cause various diseases and developmental disorders: the so-called ciliopathies.[5] Specific receptors and ion channels in the cilia membrane influence various signaling pathways responsible for development, such as Notch, Wnt, and Hedgehog, or the coupling of mechanical or chemical stimuli including growth factors.[6-11] These regulate differentiation, migration, and cell growth during development and adulthood.

It is known that many ciliopathies are associated with altered cilia lengths.[12] The length of the cilium is controlled by various proteins and mechanisms such as vesicle transfer and remodeling of the actin cytoskeleton.[13] In particular, stimulation with growth factors and the associated ligand binding to the specific receptors can influence cilia length.[14] Longer cilia may induce a greater influx of calcium ions (eg, by mechanical stimuli) because less force is required to bend the cilium.[15] In addition, the elongation also increases the volume of the cilium, which is associated with concentration modifications of ions, proteins, and signal molecules, leading to biological responses.[16] Other factors that influence the cilium length

include chondrogenic dedifferentiation processes during expansion,[17] the concentration of metal ions such as cobalt that can result from corrosion processes of implants,[18] or autophagy processes.[19]

Primary cilia are also important for cartilage health.[20] In chondrocytes, primary cilia are predominantly located in deep ciliary pockets and have lengths of about 1 µm to 3 µm (in the z-stack projection), so they generally do not extend from the cell surface.[17,21-24] In comparison, the ciliary length in osteoblasts is up to 4 µm.[25]

As the primary cilium appears to be involved in different key signaling pathways and diseases, the ability to investigate this structure efficiently and reproducibly is vital to identify mechanisms associated with this distinctive structure. The determination of cilia lengths and also the number of cilia is of interest for tissue engineering approaches or therapeutic strategies. Until now, manual image analysis approaches have predominated, although these are time-consuming, user-biased, and error-prone, and the results are difficult to compare due to the individual's interpretation of a cilium. Of 24 publications (for this overview, we examined all publications referenced in this publication [excluding reviews and tool papers] and added the first 10 results of a Web of Science search ["primary cilium" AND "length" {Topic} and 2012-2022 {Year Published}, NOT Document Types: Review Article]), authors of 21 of these publications manually detected and measured primary cilia,[8,14,15,17,18,23,24,26-39] one[21] used software to achieve this task (semi-)automatically and two[25,40] have not stated how this was done. However, we believe it was done manually because no tool was mentioned.

These studies required high-resolution imaging techniques because the primary cilium is only a few micrometers long. The ability of an imaging system to resolve these details is described by the optical resolution. It depends on the point spread function (PSF), which is the 3-dimensional representation of a single point of light imaged by a microscope.[41] In confocal microscopy, the PSF is influenced by the numerical aperture of the objective lens, the immersion medium used, the emission and excitation wavelengths, and the pinhole diameter. Using the Houston criterion,[42] the theoretical limits of the optical resolution of a confocal microscope are given by the lateral full-width half-maximum $LFWHM = 0.37 \cdot \bar{\lambda} / NA$ and axial full-width half-maximum $AFWHM = 0.64 \cdot \bar{\lambda} / \left(n^2 - \sqrt{n^2 - NA^2} \right)$ of the PSF with the mean wavelength $\bar{\lambda} = \sqrt{2} \cdot \lambda_{ex} \cdot \lambda_{em} / \left(\sqrt{\lambda_{ex}^2 + \lambda_{em}^2} \right)$—employing both the excitation $\left(\lambda_{ex} \right)$ and emission wavelengths $\left(\lambda_{em} \right)$, the numerical aperture NA of the objective lens, and the refractive index of the immersion medium n.[43] Knowing these values allows one to use suitable sampling rates.

To improve the reproducible analysis of cilia, we have developed an open-source R[44] package coined detectCilia. It focuses on automatic counting and 2-dimensional (2D)/3-dimensional (3D) measurement of primary cilia lengths in confocal microscopy images. We are using R because it is highly accepted in the scientific community, and the usage of this data science ecosystem is still increasing.[45] The tool was tested with the results of an *in vitro* study of human chondrocytes cultured in different cell culture media on collagen-coated glass surfaces. First, we used 7 test images to evaluate detectCilia by comparing its results with manual detection and length measurements performed by 3 raters as well as with 2 existing cilia detection tools: ACDC[46] and CiliaQ.[47] Second, the R package, ACDC, and CiliaQ detected and measured the cilia in all acquired microscopy images to analyze the effect of cell culture medium composition on ciliary length. We thoroughly compared the results of all 3 tools.

Materials and Methods

Cell culture

For investigating the influence of the cell culture medium composition on the lengths of primary cilia, human nondegenerative chondrocytes from a 30-year-old male donor (NHAC-kn, CC-2550; LONZA, Walkersville Inc., Walkersville, Maryland) were used. These chondrocytes were seeded in passage 4 with a density of 28 000 cells/cm² on collagen-coated glass coverslips (GG-15-Collagen; Neuvitro Corporation, Camas, WA, USA). The cells were cultivated in 12-well plates (Thermo Fisher Scientific Inc., Waltham, Maryland) under hypoxic conditions at 37°C, 5% CO_2, and 5% O_2 with different media compositions for 3 days.

The basal medium consisted of Dulbecco's Modified Eagle Medium (Gibco) including high glucose (GlutaMAX), sodium pyruvate supplements (Thermo Fisher Scientific Inc.), as well as 1% penicillin/streptomycin (Pen/Strep; Thermo Fisher Scientific Inc.), 1% amphotericin B (Biochrom GmbH, Berlin, Germany), and 50 µg/mL ascorbic acid (Sigma-Aldrich, Merck KGaA, Darmstadt, Germany). Different supplements were added to this basal medium to investigate the influence of different culture media on ciliary length, creating 4 groups:

1. ITS: 1% insulin-transferrin-selenium (ITS+ Premix; BD Biosciences, Franklin Lakes, New Jersey);
2. ITS with Dexa: 1% insulin-transferrin-selenium (ITS+) and 100 nM dexamethasone (Sigma-Aldrich);
3. ITS with Dexa + IGF-1 + TGF-β1: 1% insulin-transferrin-selenium (ITS +), 100 nM dexamethasone, 50 ng/mL insulin-like growth factor (IGF)-1 (R&D Systems, Minneapolis, Minnesota), and 50 ng/mL transforming growth factor (TGF)-β1 (Peprotec, Hamburg, Germany);
4. FBS: 10% fetal bovine serum (FBS; Pan Biotech, Aidenbach, Germany).

In the case study, the experiments of groups 1 and 4 were performed once $\left(N = 1 \right)$, and the experiments of groups 2 and 3 were performed twice $\left(N = 2 \right)$.

Immunocytochemistry

After 3 days of cultivation in the different media compositions, the chondrocytes were washed once with phosphate-buffered saline (PBS; Biochrom GmbH) and fixed for 10 minutes at room temperature (RT) with 4% paraformaldehyde (ROTI Histofix; Carl Roth GmbH + Co. KG, Karlsruhe, Germany). After fixation, cells were washed again and permeabilized with 0.2% Triton-X100 (Merck, Darmstadt, Germany) for 10 minutes. For blocking the unspecific binding sites, cell-seeded coverslips were incubated with bovine serum albumin (Sigma-Aldrich) with a concentration of 5% in PBS for 1 hour at RT after another washing step with PBS. To stain the primary cilium, cells were incubated with anti-acetylated ∝-tubulin (6-11B-1) (RRID: AB_628409) labeled with Alexa Fluor 647 (sc-23950 AF647; Santa Cruz Biotechnology, Dallas, Texas) diluted 1:200 in PBS at 4°C overnight. In addition, the actin cytoskeleton was stained with Acti-stain 488 Fluorescent Phalloidin (Cytoskeleton, Inc., Denver, Colorado) diluted 1:140 in PBS for 30 minutes at RT. Afterward, cells were washed 3 times with PBS, and the coverslips were fixed with Fluoroshield (Sigma-Aldrich) containing $4',6$-diamidino-2-phenylindole.

Image acquisition

Three-dimensional fluorescence images of stained cells were acquired with a ZEISS ELYRA LSM 780 confocal laser scanning microscope (CLSM; Carl Zeiss AG, Oberkochen, Germany). Images were recorded using a Plan-Apochromat $63 \times / 1.40$ Oil DIC M27 objective lens (Carl Zeiss AG) and Zeiss Immersol 518 F immersion oil. The z-step interval (distance between 2 consecutive z-stack layers) was 0.2814 μm and the pixel area $0.2196\,\mu m \times 0.2196\,\mu m$ with the frame size of 1024×1024 (zoom: 0.6). To compare the results depending on the pixel sizes, we have also used frames of size 2048×2048 and 4096×4096 pixels and an Plan-Apochromat $100 \times / 1.46$ Oil DIC M27 Elyra objective lens (Carl Zeiss AG) resulting in different pixel sizes. Additional metadata can be found in the original microscopy files uploaded to Zenodo (see section "Data Availability").

Image analysis: manual detection and measurement of the lengths of cilia

Images acquired with the CLSM and saved in the CZI format were processed and interpreted in Fiji[48] (Fiji is just ImageJ) (ImageJ v1.53c). Strictly speaking, the length of anti-acetylated α-tubulin was measured and used as a proxy for the cilium length. Before detecting and measuring the cilia, the brightness and contrast were adjusted using the automatic brightness/contrast adjustment function of Fiji. Afterward, the cilia were identified and numbered in a projection of the z-stack (using the maximum intensity method). Depending on the specificity of the staining, other objects, such as membranous or mitotic

structures or other fixation artifacts, were sometimes visible and had to be neglected. Therefore, a researcher labeling the cilia (manual rater) needed to differentiate between actual cilia and other objects by looking at typical features of primary cilia: brightness, length, and uniqueness per cell. Still, some images prohibited a clear identification of all (non-)cilia (see Supplemental Figure S3 for 2 examples).

Next, the horizontal lengths of the detected cilia were determined in the z-stack projection using the line tool, trying to find the maximum extension of each cilium using a straight line. Finally, the lowest and highest z-stack layers, which belong to a cilium, were found.

With these measurements, the vertical length l_z was calculated by taking the product of the difference between the topmost $\left(\text{layer\_index}_t\right)$ and bottommost layer $\left(\text{layer\_index}_b\right)$ in which a cilium appeared—adding one to include the full extension of the cilium—with the spacing of the z-stack layers $\left(d_z\right)$: $l_z = \left(\text{layer\_index}_t - \text{layer\_index}_b + 1\right) \cdot d_z$. The horizontal length l_{xy} was measured in pixels and was multiplied during the data analysis procedure with the x/y-scaling factors from the metadata. The total length of a cilium was approximated by applying Pythagoras' theorem: $l_{\text{cilium}} \approx \sqrt{l_z^2 + l_{xy}^2}$.[31] Cilia touching a border $\left(x, y, \text{ or } z\right)$ of an image were disregarded. A detailed workflow is found in section "Workflow for manually finding and measuring cilia" of the Supplemental Material.

Image analysis: using the R package detectCilia

The developed R package detectCilia (v0.8.4) will be introduced in section "R package detectCilia." In Listing 1, the main function to use this R package is shown. We used predefined (default) parameter values, such as the colors of the cilia and nuclei, and let the tool calculate missing values, such as thresholds, depending on the properties of an image. The R script to work with detectCilia and reproduce the results of this publication is found on GitHub (https://github.com/SFB-ELAINE/SI_lengthOfPrimaryCilia/).

```
1 detectCilia::detectCilia(input _ file _ czi =
"test.czi")
```

Listing 1: R function call for automatically detecting and measuring all cilia in the image file "test.czi".

For every medium composition, we have acquired several z-stack image files:

1. ITS: 6 files $\left(N = 1\right)$;
2. ITS with Dexa: 12 files $\left(N = 2\right)$;
3. ITS with Dexa, IGF, TGF: 13 files $\left(N = 2\right)$;
4. FBS: 5 files $\left(N = 1\right)$.

All detectCilia results have been manually checked. Of 797 found ciliary objects in total, 29 false positives were removed because we could not identify them as primary cilia and 26

were removed during the data analysis because they touched a z border. (For horizontal length comparison, cilia touching the z borders were not removed because the z information is unavailable when using the projection images with the other 2 tools. Cilia touching the x or y borders were already removed during the detection step of detectCilia.)

We have used 7 images from Group 2 (ITS with Dexa) for the evaluation of our tool (see section "Comparison of manual and automatic cilia detection and measurements"). These images were 190815_EV38_2_Collagen_ITSwithAsc+Dexa_ 63x_zstack_1. . .7.czi.

Image analysis: using ACDC (Automated Cilia Detection in Cells)

We have used the software for Automated Cilia Detection in Cells (ACDC) v0.93[46] to automatically detect and measure cilia in the z-stack projections of the microscopy images. Before this Matlab tool could be used, the images needed to be converted because ACDC detects cilia in the green channel. (We applied a red fluorescent dye to label the cilia.) For this, all images were converted to TIF files, using the maximum intensity z-stack projection and switching the information of the red and green channels such that the cilia may be detected in the green channel using the function convertCziToTif from our R package readCzi (https://github.com/SFB-ELAINE/readCzi) (v0.4.1). The function for image and channel conversion is shown in Listing 2.

```
1 readCzi::convertCziToTif(input_file = "test.
czi", change_layers = "red<->green",
projection_method = "max",
higher_contrast_projection = FALSE,
normalize_projection = FALSE, add_scale_bar
= FALSE)
```

Listing 2: R function call to convert a CZI file to TIF and change color layers of the image file "test.czi."

The ACDC requires 5 parameter values to detect and measure cilia automatically. To find the best combination, we analyzed the first image from each sample stack (8 images in total). We used the following parameter values: Kernel length: 200, SNR Threshold: 1.4, Min cilia length: 0, Directional threshold: 0.3, Standard deviation threshold: 0, and manually labeled missing cilia and removed false positives in every image. (These values were previously found after labeling the 7 test images from Group 2.) In the end, we used the auto-optimization method for finding parameter values achieving the highest precision (Precision: 0.804, Recall: 0.650, F1 Score: 0.719): Kernel length: 200, SNR Threshold: 1.73, Min cilia length: 0, Directional threshold: 0.41, Standard deviation threshold: 0. We used these values to detect cilia in all images without correction but also with correction, adding missed primary cilia (false negatives) and deleting false positives. The correction was necessary because ACDC usually requires that "for each

experimental paradigm, the settings need to be optimized before analysis."[46]

Image analysis: using CiliaQ

CiliaQ[47] constitutes a 3-step workflow based on 3 ImageJ plugins: (1) CiliaQ_Preparator (v0.1.2) prepares the images for segmentation and segments the images into cilia and background; (2) CiliaQ_Editor (v0.0.3) allows manual corrections of the segmentation; and (3) CiliaQ (v0.1.7) automatically reconstructs the cilia, quantifies them, and visualizes the results.

In the case study, we used the original 3D CZI files as well as the same 2D TIF images as for ACDC. Before we could use the plugin, the 2D images had to be converted to RGB stacks in ImageJ (Image $\rightarrow$ Type $\rightarrow$ RGB Stack). Next, CiliaQ_Preparator was used for segmentation, applying the default parameter values everywhere except for the channel number: 2, segmentation method: "triangle," and segmentation style: "Set intensities above thresholds to maximum possible intensity value." Finally, the segmented images were analyzed using CiliaQ with the following parameter values: Calibration [unit / pixel] = 0.219647, Voxeldepth [unit / voxel] = 0.281399, Calibration unit: "µm," Channel for reconstruction: 2, in addition exclude: "cilia touching x or y (or z) borders" (z border only for 3D images), Minimum cilium size [voxel]: 5, Gauss filter before skeletonization XY sigma: 0.0, Z sigma: 0.0. We experienced that a Gaussian filtering value larger than zero before skeletonization significantly reduces cilia lengths. Therefore, we changed the default value from 2 to 0. In addition, we manually checked all CiliaQ results. We removed false positives by looking at the images of the found cilia and excluded those that did not appear to be ciliary objects. False negatives were not corrected because most cilia were found, and it would have been a time-consuming task compared with the approach used by ACDC.

Statistics

When comparing different experimental groups, we first tested for normal distributions of the cilia lengths using the Shapiro-Wilk test. The null hypothesis of a normal distribution was not rejected when $P > .05$. As we always had at least one group showing a non-normal distribution, we used the Wilcoxon signed-rank test (with Bonferroni corrections when comparing more than 2 groups). The adjusted P values are shown as significance levels in the corresponding plots. Please note that we compare cilia lengths from 2 replications $(N = 2)$ of the *in vitro* experiments in groups 2 and 3 and 1 replication $(N = 1)$ of the experiments in groups 1 and 4. We have pooled the replication results of groups 2 and 3 even though we found a statistically significant difference in group_2 (ITS with Deca) for the total lengths $(P = 0.02,\ \bar{l}_2 = (3.89 \pm 0.14)\,\mu\text{m},\ \bar{l}_3 = (3.68 \pm 0.12)\,\mu\text{m}$. All statistics were calculated in R. (See section "Data Availability" for information about reproducing the results.)
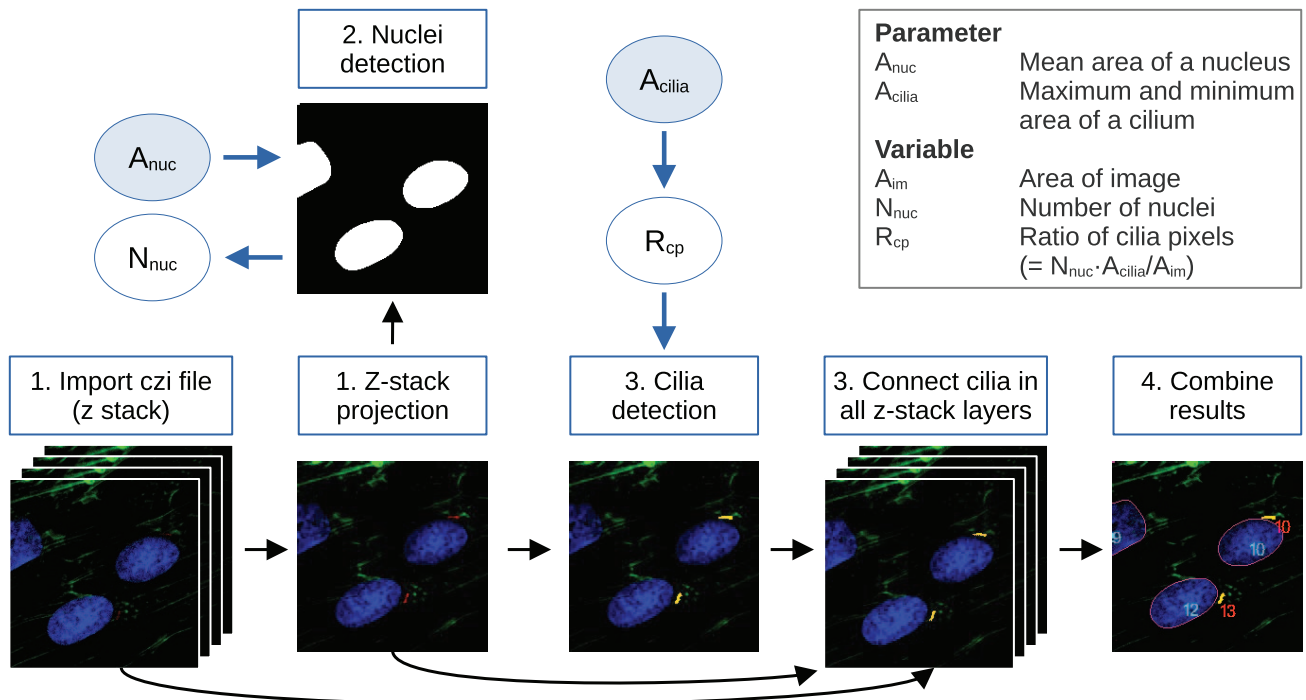
Figure 1. Default workflow of detectCilia. 1. Image preparation: The original microscopy files are imported, and, if applicable, a maximum intensity z-stack projection is calculated. 2. Nuclei detection: The stained nuclei are segmented and counted using the mean area of a nucleus as an input parameter. 3. Cilia detection: Cilia are detected in the z-stack projection and every z-stack layer using the ratio of possible cilia pixels. Here, a primary cilium's (expected) area is needed as an input parameter. 4. Cilia measurement: The information on all cilia (eg, lengths and heights) is collected, and the total lengths are calculated. The results are saved in a CSV file. (The images shown are sections of `190815 _ EV38 _ 2 _ Collagen _ ITSwithAsc+Dexa _ 63x _ zstack _ 3.czi` with enhanced brightness and contrast for better visualization.)

Results and Discussion

First, we present the developed R package. Then, we compare detectCilia with ACDC and CiliaQ and evaluate the package using simulated cilia and the test images of the case study. Finally, we show and discuss the impact of different media compositions on the lengths of primary cilia of human chondrocytes.
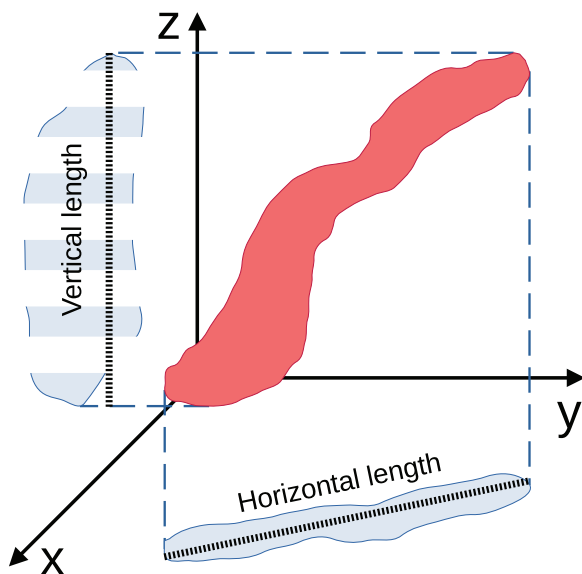
R package detectCilia

We have developed an open-source R package called detect-Cilia (the package is found on GitHub: https://github.com/SFB-ELAINE/detectCilia) to automatically detect and measure cilia in (confocal) fluorescence microscopy images. It can work with either TIF or CZI (Zeiss) files. The latter is preferred because exported TIF files may have been manipulated (eg, changed brightness/contrast) and may lack important metadata. Functions to work with image data from other confocal fluorescence microscopy manufacturers (eg, ND2 [Nikon], LIF [Leica], or OIF [Olympus]) will be included in the future.

detectCilia imports and uses the following packages: BiocManager,[49] devtools,[50] reticulate,[51] and dplyr.[52] BiocManager is used to install the R package EBImage;[53] devtools is used to install our own package readCzi[54] that is currently available on GitHub; and reticulate is used to install the Python library czifile[55] needed to read CZI files. Details on the complete functionality of the R package are found in section "R package detectCilia" of the Supplemental Material. In general, the main function of the package, *detectCilia()*, is a 4-step process, described in the following and visualized in Figure 1.

1. Image preparation: The file (either in CZI or TIF format) is imported into R as a 3D or 4D array $(x, y, (z),$ and color channel). Next, a z-stack projection is calculated. We have compared the average and maximum intensity projection methods and decided to use the latter by default because it is more reliable, especially when, otherwise, averaging many z-stack layers would lead to a low signal-to-noise ratio.

2. Nuclei detection: We apply different methods from the EBImage package to find, label, and count nuclei (ie, *thresh()*, *opening()*, *fillHull()*, *bwlabel()*).

3. Cilia detection: First, the thresholds for finding cilia in the z-stack projection and in every layer are calculated if these are not passed as arguments to the function. The thresholds are calculated by looking at the nth quantile of cilia pixel intensities where $n = 1 - R_{cp}$ and R_{cp} is the

Figure 2. Determination of the ciliary length. Our R package detectCilia uses the maximum extension of the z-stack projection for calculating the horizontal length. The vertical length is calculated by counting the number of z-stack layers where parts of a cilium can be seen. This number is multiplied by the spacing of the layers. The total length is calculated using Pythagoras' theorem.

ratio of cilia pixels. This ratio can be calculated by multiplying the number of cells with the expected cilium area in pixels divided by the frame size of the image. Second, a binary image is being created depending on the threshold. Third, this binary image of possible cilia is cleaned to remove false positives by (1) deleting pixels without direct neighbors, (2) combining ciliary objects that are close to each other, (3) deleting pixels with too low intensities, (4) deleting structures that are either too large or too small, and (5) deleting all separated substructures of a possible cilium that are not directly connected to the brightest pixel of the particular cilium. Last, we find corresponding cilia pixels in other z-stack layers.

4. Cilia measurement: For every image, a CSV file with each cilium's length and height measurement and the calculated total length is saved (cf. Figure 2). Furthermore, a CSV containing the number of identified nuclei and a CSV file containing the passed function arguments are saved. In addition, TIFs containing the labeled nuclei and cilia are created.

A few assumptions have been made to automatically calculate parameter values for the detection step, which are used when the user does not enter specific detection parameter values. We assume that

1. Every cell contains 1 nucleus and, at most, 1 primary cilium.

2. The projected area of a cilium (z-stack projection) is between 1 μm × 0.25 μm and 5 μm × 1 μm.
3. The nucleus area is in the order 15 μm × 15 μm.

These assumptions are used in the calculation of the threshold values for detecting cilia in the z-stack projection (*threshold_find*) and for connecting cilium points of other z-stack layers to the found cilia (*threshold_connect*) if the thresholds are not explicitly given by the user. The calculated thresholds depend on the ratio of (possible) cilia pixels. For this, the number of nuclei (and thus cells) in an image is needed. The ratio is then used to determine the thresholds by calculating the corresponding quantile of the pixel intensity distribution. The exact calculations are found in section "Input parameters of the main function *detectCilia()*" of the Supplemental Material.

Comparison of detectCilia with the similar cilia measurement tools ACDC and CiliaQ

Before we evaluate the R package, we compare it with the currently available tools for detecting and measuring cilia: ACDC[46] and CiliaQ.[47] Similarities and differences between the tools are summarized in Table 1.

Although each tool is written in another programming language (ACDC in MATLAB, CiliaQ in Java, and detectCilia in R), the 3 tools use similar methods to detect and measure cilia. They all apply segmentation algorithms using (adaptive) thresholds and some cleaning methods to differentiate between true-positive cilia and false-positive cilia. However, the tools differ in various ways when looking at the details.

The detection of cilia in detectCilia is wholly automated without the requirement of changing default parameter values, although the user may specify all values explicitly. The segmentation thresholds in detectCilia depend upon the number of found nuclei, as 1 primary cilium per cell may occur. Users of CiliaQ may choose among different segmentation methods based on threshold methods implemented in ImageJ, which leads to different results for both the number and length of cilia. The ACDC permits the user to change the parameter length kernel, which influences the number and size of the segmented objects. We observed that a higher length kernel value led to the detection of many short nonciliary objects. Both ACDC and CiliaQ need specific parameter values for filtering the results. These 2 tools also allow manual corrections of the segmented cilia.

detectCilia does not skeletonize the found cilia, thus ignoring possible curvatures and branches of the detected ciliary objects. Instead, it calculates the longest distance of any 2 pixels belonging to the same object in the *xy* -plane and its height. We believe that the bending of a cilium is random; thus, ignoring it underestimates the true cilia lengths but does not influence the result of comparing the mean cilium lengths of

Table 1. Similarities and differences between detectCilia, ACDC, and CiliaQ.

FEATURE	DETECTCILIA	ACDC	CILIAQ
Detection mode	Automatic	Manual or automatic with possibility for manual corrections	Automatic with possibility for manual corrections
Valid image dimensions	2D, 3D	2D	2D, 3D, 4D (= 3D + time)
Data input format	CZI, TIF	TIF, JPEG	All common formats (using the Bio-Formats plugin for ImageJ)
Skeletonization of cilia	No	Yes	Yes
z-stack projection method	Maximum (as default) or mean intensity	—	Maximum intensity
Segmentation parameter values	Automatically or manually set	Manually and automatically set[a]	Automatically set with the choice of different segmentation methods
Filter parameter values	Automatically set	Manually set	Manually set
Cell count (stained nuclei)	Yes	Yes[b]	No
Programming language	R	MATLAB	Java
Graphical user interface	No	Yes	Yes
Open-source	Yes	No	Yes
Reproducible image analysis	Yes	Yes[c]	Yes[c]

[a]After manually labeling a representative image, the post-processing parameter values may be chosen automatically by an optimization algorithm.
[b]The cell count did not work correctly in our case.
[c]Only if no manual corrections are made and all used parameter values are published.

different groups. As seen in section "Bending indices of cilia" of the Supplemental Material, this might only be true for cilia in the z-stack projections. However, we could not locate literature examining the impact of different conditions on the curvatures of primary cilia.

Another difference is the usage of open-source software, which enhances transparency, fosters reproducibility, and facilitates its application. Only CiliaQ and detectCilia are open source. Furthermore, ACDC is constrained to 2D images, making estimating the total length difficult. In addition, it uses the same post-processing segmentation parameter values for all images of a set, which requires the same quality for all images.

Some of these differences lead to different degrees of reproducibility because ACDC and CiliaQ will produce reproducible results only when all input parameter values are manually recorded, and no manual corrections are done. Although initially detectCilia might appear less intuitive without a GUI than the other 2 tools, it ensures reproducible results by explicitly recording all (default or manual) input parameter values.

The efficacy of the 3 tools can best be tested with simulated cilia. As ACDC can only work with 2D data, we let the tools determine the horizontal length of a simulated cilium convolved with a 2D Gaussian kernel (Gaussian filter/Gaussian blur), mimicking a microscope's PSF (see Introduction). The measured lengths depending on the Gaussian filter standard

deviations are seen in Figure 3. A Gaussian function has an FWHM of $2\sqrt{2\ln 2}\sigma \approx 2.36\sigma$. Therefore, a standard deviation σ of one pixel with a pixel size of 0.22 would be equivalent to a lateral FWHM of the PSF of 0.52 µm, which is about 3 times larger than the calculated lateral FWHM of our used imaging system (see "Comparison of manual and automatic cilia detection and measurements"). All 3 tools detected the cilium within the blurring range when each cilium is in a separate image, as seen in Figure 3A. In this case, detectCilia has determined the correct size of the cilium until the standard deviation has reached 2.5 pixels. From this value onward, the horizontal lengths were measured slightly shorter because of lower contrasts. On the contrary, CiliaQ has not determined the correct size once because the skeletonization algorithm decreases the length of an object depending on its width.[56] The length of the cilium has also increased with more blurring because more non-black pixels filled the image. ACDC's length measurement was less predictable because the ridge detection works differently from the skeletonization and sometimes adds additional curvatures.

When the 50 cilia with Gaussian blur standard deviation values from 0.0 to 4.9 pixels were combined in one image (cf. Supplemental Figure S10), the tools produced slightly different results, as seen in Figure 3B. The results of CiliaQ were identical to the isolated cilia detection. The horizontal lengths
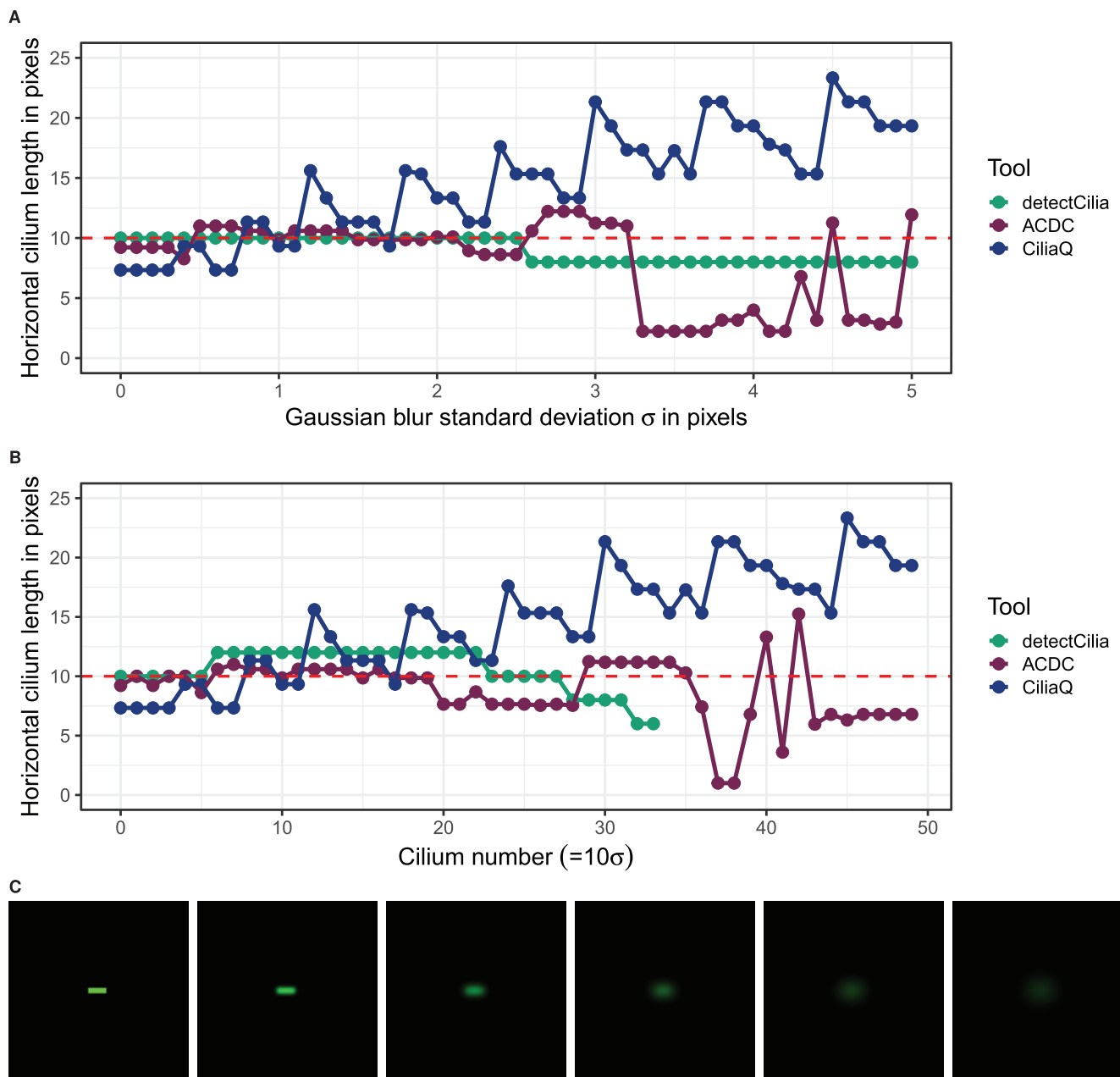
Figure 3. Simulated cilia with a length of 10 pixels and a width and height of 3 pixels with added Gaussian blur were measured by all 3 tools. (A) and (B) show the results of the horizontal length measurements. In (A), the cilia with added Gaussian blur were detected and measured individually (1 cilium per image). In (B), the images with the blurred cilia were combined; therefore, one image containing all cilia (except for the cilium with an added blur of $\sigma = 5$ pixels) was used for detection and measurement. (The cilium number divided by 10 corresponds to the Gaussian blur standard deviation in pixels used for that particular cilium.) The results of CiliaQ are identical for both approaches. (C) Images of the z-stack projection of the simulated cilium with Gaussian blur standard deviation values 0, 1, 2, 3, 4, and 5 pixels (from left to right).

determined by ACDC and detectCilia were similar, although detectCilia disregarded all cilia blurred with $\sigma > 3.3$ pixels. detectCilia applies the same threshold in the entire image and uses minimum and maximum values for cilium sizes to minimize false-positive cilia. Therefore, the tool has disregarded the smeared-out cilia.

The impact of the orientation of a cilium in 3D on the length measurements was also examined. As seen in section "3D length measurement of a c-shaped simulated cilium" of the Supplemental Material, the measured lengths of a c-shaped simulated cilium are similar to the calculated lengths. However, deviations of up to 2 pixels (about 20%) can occur depending

A

B   **C**
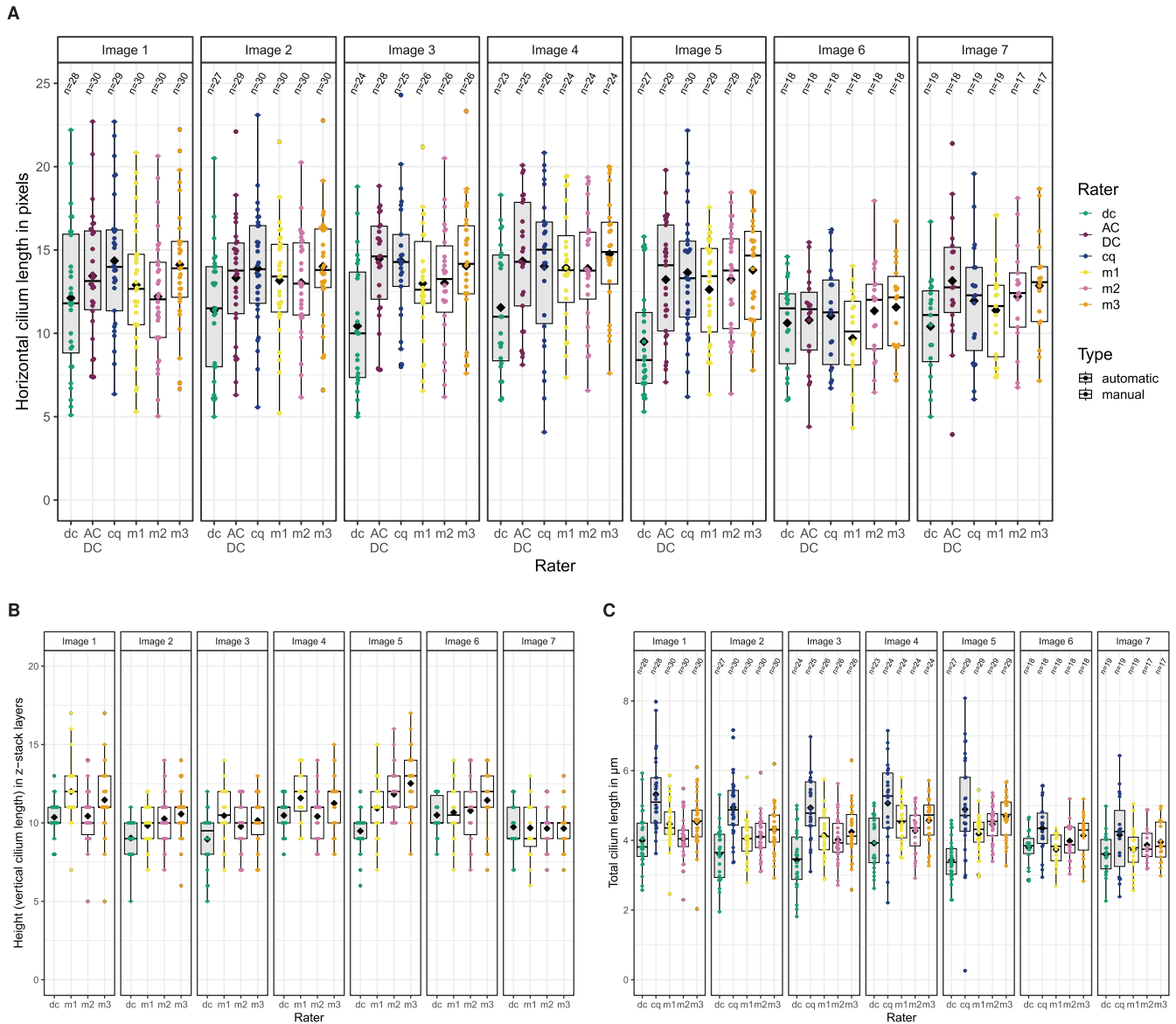
Figure 4. Results of automatic and manual detection and measurement of cilia in the 7 test images from the ITS with Dexa group. (A) Horizontal length (in pixels) measured in z-stack projection by all 3 tools and 3 raters. (The size of one pixel in x-direction and y-direction is 0.2196 µm). (B) Vertical length (in z-stack layers) determined by the distance from the lowest to the highest z-stack layer containing pixels belonging to a specific cilium. (The z-step interval is 0.2814 µm.) (C) Total length (in µm) of every cilium in every image. Note that CiliaQ used the z-stack projection images for horizontal length measurements and the original CZI files for the total lengths, resulting in slightly different numbers of detected cilia. All box-and-whisker plots are shown with median, first and third quartiles, outliers, as well as the mean values (black diamonds).
cq indicates CiliaQ; dc, detectCilia; m1 to m3, 3 independent manual raters.

on the specific orientation. These discrepancies are primarily attributable to rounding effects in the calculation of voxel positions during the rotation of the cilium.

To estimate the effectiveness of the tools, we compared the detection and measurement results from ACDC, CiliaQ, detectCilia of the 7 test images of the case study (`190815_ EV38_2_Collagen_ITSwithAsc+Dexa_63x_ zstack_1...7.czi`) (see Figure 4A and C of section

"Comparison of manual and automatic cilia detection and measurements"), it becomes clear that both the number of detected primary cilia as well as their lengths vary from tool to tool, but are still in good agreement. However, we used the semi-automatic detection mode of ACDC and removed false-positive cilia from the CiliaQ results to get comparable results. For the 7 test images, we manually added 48 (false-negative) and removed 16 (false-positive) cilia in total in ACDC, and

manually removed 4 and 6 (false-positive) cilia from the results of CiliaQ from 2D and 3D results, respectively. No false-positive cilium had to be removed (from the detectCilia results).

Comparison of manual and automatic cilia detection and measurements

We have used the images `190815_EV38_2_Collagen_ITSwithAsc+Dexa_63x_zstack_1...7.czi` (7 images in total) of the case study to evaluate the effectiveness of detectCilia. Cilia were detected in every image manually by 2 independent raters and automatically by our R package, ACDC, and CiliaQ. Rater *m1* detected in total 174 cilia and rater *m2* 172 cilia, whereas the R package found 166 cilia. Both ACDC and CiliaQ detected 177 true-positive primary cilia, thus some more than the independent manual raters. Distinguishing true and false positives is an ambiguous task, so we have not calculated F1 scores because it is unfeasible to establish a ground truth from these images.

The length of each cilium was manually determined by 3 independent raters (*m1*, *m2*, *m3*) and automatically by the 3 tools. (Rater *m3* has used the detected cilia of *m2* to measure lengths.) The results are shown in Figure 4. The individual lengths of every detected cilium are presented in Supplemental Figures S4 and S5.

As seen in Figure 4A, the median horizontal lengths of the z-stack projections differ by 0 to 5 pixels between automatic (gray boxes) and manual measurements (white boxes). The median values within the manual detection group differ by 0 to 2 pixels. The largest deviation between manual and automatic results is seen for detectCilia in images 3 and 5. detectCilia occasionally underestimates the length of a cilium when it is darker than most other cilia in an image.

The vertical length measurements also show disagreement among the raters, as shown in Figure 4B. detectCilia accounts for 0 to 2 fewer z-stack layers. The height results could not be compared with the results of CiliaQ as the tool does not save the z-stack layers of a cilium.

As a consequence, the median values of the total lengths are slightly smaller for the detectCilia results compared with the manual measurements, as seen in Figure 4C. On the contrary, CiliaQ has determined the total cilia lengths to be larger compared with the results of the manual raters. Most likely, this is because CiliaQ skeletonizes found cilia and, therefore, incorporates curvatures of cilia which are primarily present in z-direction, whereas both detectCilia and the manual raters linearize the cilia.

When a cilium extends for approximately 12 pixels, a deviation by 2 pixels already imposes a large error. Therefore, one could try to minimize the error by using a higher digital resolution. However, a higher sampling rate (lower pixel size) by using a larger frame size, zoom factor, or magnification will not necessarily lead to better results in total because it is not the magnification or frame size that influences the resolving power of the system.[41] As seen in the Introduction, the optical resolution of a microscope depends on the PSF.

With our data of the cilium channel $\left(\lambda_{ex} = 633\text{nm} \lambda_{em} = 697\text{nm}, NA = 1.4, n = 1.518\right)$, we get, as an estimate of the PSF, LFWHM $\approx 0.18\mu m$ and $\approx 0.25\mu m$. According to the Shannon-Nyquist sampling criterion, the pixel size needs to be at least 2 times smaller than the optical resolution to get a sufficient representation of the specimen.[57,58] Using larger pixel sizes may lead to aliasing, which causes objects to appear smaller, larger, or in the wrong locations.[59] We applied slightly suboptimal spacing, but the cilia we tried to detect were about 3 µm in size, and, therefore, the advantages of using a higher sampling rate did not outweigh its disadvantages, as seen in section "Impact of the pixel size on detectCilia results" of the Supplemental Material.

Case study: influence of medium composition on the cilium length

Human chondrocytes were cultured in different cell culture media to analyze the influence of the medium composition on the lengths of primary cilia. Figure 5 shows the cilia lengths determined by detectCilia depending on the used cell culture medium. The results are summarized in Table 2. Significant differences in the cilia lengths could be observed. Cartilage cells in basal medium with ITS and with or without dexamethasone possessed the longest cilia with a total length of about (3.8 ± 0.1) µm. Significantly shorter cilia were detected in cells cultured in basal medium containing additional ITS, dexamethasone, and the growth factors IGF-1 and TGF-β1 ([3.34 ± 0.08] µm) and in medium containing FBS ([3.18 ± 0.10] µm).

Interestingly, the number of cells found in the FBS group was about 2 times higher than in the 3 other groups (50 cells instead of 25 cells per image). This shows that FBS has led to enhanced proliferation, which is expected because FBS contains different growth factors and many other compounds that support proliferation.

As seen in Table 3, the assumptions required by detectCilia to automatically detect cilia (see section "R package detectCilia") were also met. The mean nucleus area was in the order of 15 µm × 15 µm and between 65% and 84% of the cells had primary cilia that were stained and detected.

We have also evaluated all case study images with the 2 other tools. The measured horizontal cilia lengths determined by the 3 tools are shown in Figure 6A. In all groups, ACDC measured primary cilia to be about 0.5 µm longer than those measured by detectCilia. The results of the horizontal length measurement between detectCilia and CiliaQ were only different in the ITS with Dexa group, which is consistent with our observations from the 7 test images being from the same group. Still, the differences between the experimental groups are similar for all 3 analysis tools (see Supplemental Figure S13 for the
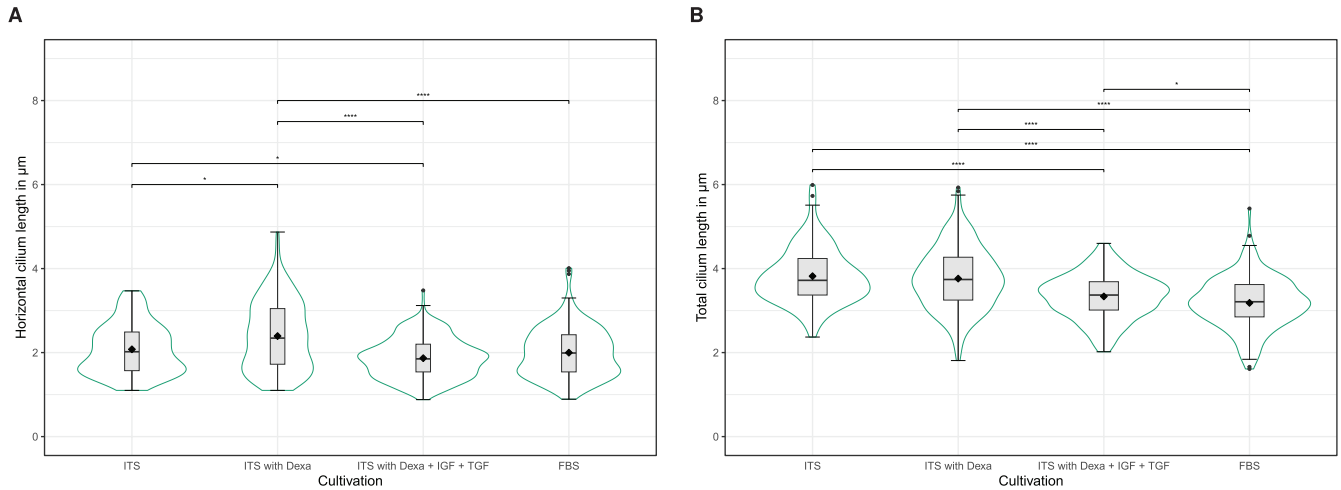
Figure 5. Length of primary cilia measured by detectCilia depending on the media compositions. (A) Horizontal lengths from z-stack projections, (B) total lengths. Box-and-whisker plots, mean values (black diamonds), and violin plots are shown.
Dexa indicates dexamethasone; FBS, fetal bovine serum; IGF, insulin-like growth factor; ITS, insulin-transferrin-selenium; TGF; transforming growth factor.
Significance levels: $^{****}P < 10^{-4}, ^{***}P < 10^{-3}, ^{**}P < 10^{-2}, ^{*}P < .05$.

Table 2. Results of the automated detection of primary cilia in 36 images by detectCilia.

ADDITIONAL MEDIUM COMPONENTS	N_{Images}	n_{Cells}	n_{CILIA}	$\bar{l}$ in µm	σ_l in µm	95% CI in µm
ITS	6	150	101	3.82	0.66	$\bar{l} \pm 0.13$
ITS with Dexa	12	328	273	3.76	0.74	$\bar{l} \pm 0.09$
ITS with Dexa + IGF + TGF	13	346	194	3.34	0.54	$\bar{l} \pm 0.08$
FBS	5	231	167	3.18	0.61	$\bar{l} \pm 0.10$

The number of used images per group $\left(N_{Images}\right)$, the total number of detected cells $\left(n_{Cells}\right)$, the corrected total number of detected cilia $\left(n_{Cilia}\right)$, the mean total length $\left(\bar{l}\right)$, the standard deviation of the total length $\left(\sigma_l\right)$, and the 95% confidence interval (CI) of the mean length are shown. The 95% confidence intervals were calculated using $1.96 \cdot \sigma_l / \sqrt{n_{Cilia}}$.

Table 3. Comparison of assumptions required by detectCilia and detection results.

ADDITIONAL MEDIUM COMPONENTS	MEAN NUCLEUS AREA in µm²	MEAN CILIUM PROJECTION AREA in µm²	CILIATED CELLS IN %
ITS	11.9×11.9	1.9	67
ITS with Dexa	12.8×12.8	1.9	84
ITS with Dexa + IGF + TGF	14.1×14.1	1.5	65
FBS	13.9×13.9	1.5	72

The assumptions were nucleus area in the order of $15\,\mu m \times 15\,\mu m$, cilia projection area between $0.5\,\mu m^2$ and $5\,\mu m^2$, and (at most) 1 cilium per cell. Note that cilia touching a *z* border were included in this table.

manually corrected results and Supplemental Figure S14 for the uncorrected results). The measured total cilia lengths determined by the 2 capable tools are shown in Figure 6B. The ITS with Dexa group stands out again.

Whether the results of ACDC or CiliaQ are closer to the true cilia length cannot be said because the authors of CiliaQ have not compared the results of the tool with manual length measurements but used their tool to correct/edit the cilia masks
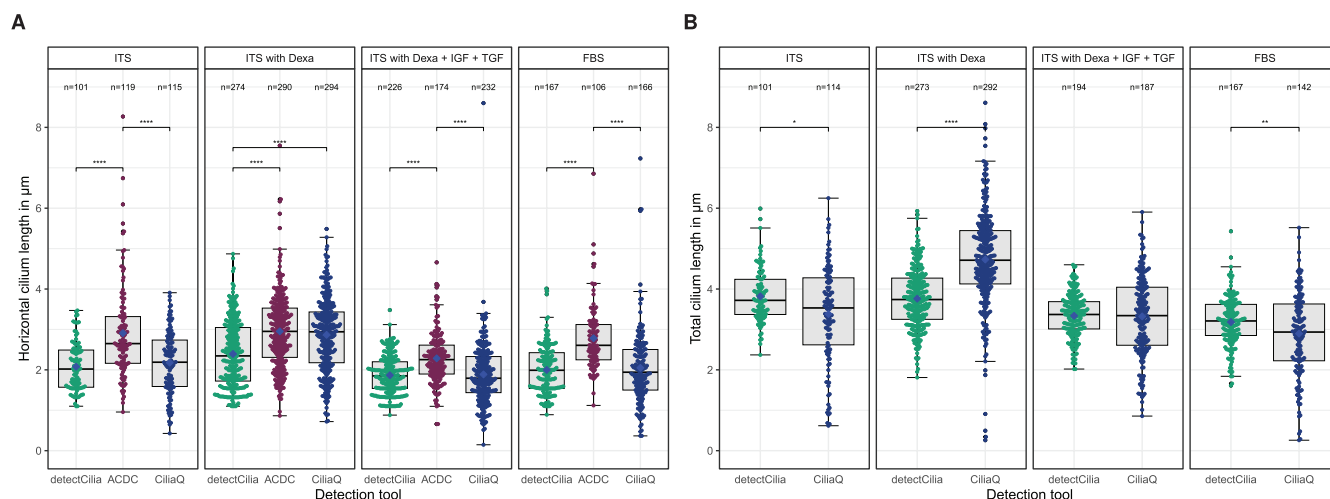
Figure 6. Number of detected primary cilia and (A) horizontal lengths as measured by detectCilia, ACDC, and CiliaQ as well as (B) total lengths as measured by detectCilia and CiliaQ depending on the media compositions. Note that cilia detected by detectCilia touching a z border were removed here. Box-and-whisker plots, mean values (blue diamonds), and individual cilia lengths are shown.
Dexa indicates dexamethasone; FBS, fetal bovine serum; IGF, insulin-like growth factor; ITS, insulin-transferrin-selenium; TGF, transforming growth factor.
Significance levels: ****: $p < 10^{-4}$, ***: $p < 10^{-3}$, **: $p < 10^{-2}$, *: $p < 0.05$.

Table 4. Number of found cilia depending on the tool.

ADDITIONAL MEDIUM COMPONENTS	DETECTCILIA			ACDC				CILIAQ (2D)		
	AUT.	FP	n_{CILIA}	AUT.	FP	FN	n_{CILIA}	AUT.	FP	n_{CILIA}
ITS	102	1	**101**	90	25	54	**119**	129	14	**115**
ITS with Dexa	274	0	**274**	249	34	75	**290**	308	14	**294**
ITS with Dexa + IGF + TGF	238	12	**226**	141	13	82	**174**	365	133	**232**
FBS	183	16	**167**	126	79	59	**106**	297	131	**166**

Aut. corresponds to the number of automatically determined cilia by the specific tool. FP stands for the number of false positives, and FN the number of false-negative cilia. n_{Cilia} is the corrected number of cilia used for further analyses. Note that cilia detected by detectCilia touching a z border were not removed for this table.

manually. Similarly, the authors of ACDC have used ACDC for manual detection and measurement. However, it is unclear whether the detected ridge was corrected when necessary.

Another observation was that the number of detected cilia differed between the 3 tools. The concrete results are shown in Table 4. One can observe that detectCilia had the best detection rate for the images of the case studies.

detectCilia found the total lengths of the primary cilia to be between 3 μm and 4 μm. Kunova Bosakova et al[14] observed 3D cilia lengths of human fibroblasts of more than 2 μm, which were elongated after treatment with FGF-2 in a time-dependent manner to more than 3 μm. The exact mode of finding the lengths was not described, but we assume that the authors have fitted a straight line in the tool View5D by Rainer Heintzmann. When just looking at the horizontal lengths (determined in the z-stack projections) as seen in Figure 6A, we obtain results similar to those by Wann and Knight,[24] who found a mean primary cilium length of about 2 μm in chondrocytes. In another study,

McGlashan et al[26] reported that the lengths of primary cilia of human chondrocytes ranged from 1.1 μm to 1.5 μm depending on the zonal location within the cartilage tissue.

In the case study, we observed the longest primary cilia in cells cultivated with ITS alone or ITS with dexamethasone. The results of detectCilia showed that the administration of IGF-1 and TGF-β1 to the cell culture medium resulted in a shortening of the cilia compared with ITS with or without the addition of dexamethasone. As it is known that primary chondrocytes in monolayer cell cultures tend to dedifferentiate and thus change toward a fibroblastic phenotype,[60-64] this could explain the different lengths of the primary cilia. In our previous work, we demonstrated that the redifferentiation of human dedifferentiated cartilage cells can be induced by IGF-1 and TGF-β1.[62,65,66]

In particular, the addition of TGF-β1 could have an impact on the shortening of the cilium length due to the accumulation of receptors at the base of the cilia. A study with

human fibroblast cell cultures showed that TGF-β receptors accumulated at the cilia base regions, which were enriched with SMAD4 after ligand stimulation.[10] As a result, the receptors were internalized by endocytosis at the ciliary pocket to activate SMAD2/3. Consequently, this led to a shortening of cilia and a reduction of ciliated cells.[67]

In contrast, stimulation with IGF-1 induces the differentiation of human mesenchymal stem cells into adipocytes via an elongation of the primary cilia, which is associated with the recruitment of IGF-1 receptors to the cilia.[29] Dalbay et al[29] stated that an increase in cilia length may be related to the addition of dexamethasone to the differentiation media, which was confirmed by the studies of Forcioli-Conti et al.[30] However, the absence of TGF-β3 in the chondrogenic differentiation medium also increased the ciliary length, whereas the addition of insulin decreased it.[29]

The cell culture study showed a decrease in length when FBS, which naturally contains different growth factors, was added to the cultivation medium.[68] Presumably, the large number of undefined factors in FBS might lead to a significant shortening, proving that the concentration and interaction of growth factors have a decisive influence on the fine-tuning of cilia length and the resulting tissue-specific differentiation capacity of the cells.

Conclusions

Primary cilia are involved in various key cell signaling pathways. Alterations in cilium length or incidence can be correlated with the cell type (also regarding [de]differentiation) or ciliopathies. As the length of the primary cilium determines its flexibility and influences its sensitivity to extracellular physical or chemical cues, it is necessary to measure this structure as accurately and as reproducible as possible. As often done, manual evaluation is very time-consuming and not reproducible because human perception differs from person to person, leading to varying results.

Therefore, we have developed the open-source R package detectCilia to detect and measure primary cilia automatically. In contrast to other tools such as ACDC or CiliaQ, the R package does not rely on custom input parameter values but uses metadata of the microscopy image as well as the number of nuclei, which are also detected if stained and distinguishable, to determine threshold parameters. In addition, the possibility of manually changing the input parameter values still exists, which makes detectCilia suitable for detecting any small, distinct objects in confocal microscopy images.

We have tested the R package with straight and curved simulated cilia and compared the results with the 2 cilia detection tools, ACDC and CiliaQ. The length measurements obtained with detectCilia were, in principle, more reliable than those of the other 2 tools in 2D and 3D. In addition, we have used 7 confocal microscopy images of human chondrocytes cultured on collagen-coated glass surfaces in a medium containing ITS with dexamethasone to compare the approaches. Primary cilia were detected and measured manually and with the 3 tools. The results achieved with detectCilia, ACDC, and CiliaQ were in good agreement with the manual measurements. However, detectCilia tended to underestimate the cilium length for some images, and CiliaQ appeared to overestimate the total lengths of cilia. These results show that detectCilia works best when the cilia staining is homogeneous. To reduce the impact of inhomogeneities in the image, we plan to include contextual regions in which cilia are detected independently in the future. In addition, even though we have found that neglecting curvatures of cilia does not distort the length measurements, we plan to include a skeletonization feature to get yet another possibility to determine the cilium length.

In the case study, we intended to analyze the influence of cell culture medium composition on the lengths of primary cilia. Culturing the cells with ITS and with or without dexamethasone led to the longest primary cilia. Adding growth factors or FBS to the medium reduced their lengths. This was true when considering the result of detectCilia. CiliaQ showed a substantial increase in cilium length in the medium containing ITS and dexamethasone and a decrease only in the FBS group. Contrary to this, ACDC found a decrease in the horizontal cilium length only when the growth factors were added to the medium. Strikingly, the false-positive rate was much higher for ACDC and CiliaQ compared with detectCilia when considering the cilia detection results of all case study images. As the results of all 3 tools do not exactly match and the sample size is too small, we cannot say which tool deviates the least from the true cilia lengths. Therefore, we may only conclude that incubating with growth factors (serum-free or included in FBS) may shorten primary cilia of human nondegenerative chondrocytes within 3 days of cultivation. In the future, we will use more samples from different donors to investigate whether our findings are generalizable.

As detectCilia led to good and easily reproducible results even if the signal-to-noise ratio was low (cf. Supplemental Figure S3), we find it to be a reliable tool. Still, face validation should be done for all tools to at least exclude nonciliary objects (false positives). In conclusion, detectCilia offers a good opportunity to detect and measure primary cilia automatically and could be used in further studies to examine mechanisms of this structure or to derive specific stimulation parameters (eg, for the regeneration of cartilage tissue).

Author Contributions

Kai Budde-Sagert: Conceptualization, methodology, software, validation, formal analysis, investigation, data curation, writing—original draft, writing—review & editing, visualization, project administration. **Simone Krueger:** conceptualization, investigation, resources, writing—original draft, writing—review & editing, project administration. **Clemens**

Data Availability

The developed R package detectCilia is available on GitHub (https://github.com/SFB-ELAINE/detectCilia).[69] All main microscopy image files can be found in Zenodo.[70] In addition, the microscopy image files used in section "Impact of the pixel size on detectCilia results" of the Supplemental Material can also be found in Zenodo.[71] The R script to reproduce the results of this publication is found in another GitHub repository (https://github.com/SFB-ELAINE/SI_lengthOfPrimaryCilia/). The analysis workflow utilizes the following R packages (or package collections): coin (v1.4-2),[72] devEMF (v4.1-2),[73] EnvStats (v2.7.0),[74] ggbeeswarm (v0.7.1),[75] ggpubr (v0.5.0),[76] rquery (v1.4.9),[77] rstatix (v0.7.1),[78] scales (v1.2.1),[79] and tidyverse (v1.3.2).[80]

SUPPLEMENTAL MATERIAL

Supplemental material for this article is available online.

REFERENCES

1. Satir P, Christensen ST. Overview of structure and function of mammalian cilia. *Annu Rev Physiol*. 2007;69:377-400. doi:10.1146/annurev.physiol.69.040705.141236
2. Satir P, Pedersen LB, Christensen ST. The primary cilium at a glance. *J Cell Sci*. 2010;123:499-503. doi:10.1242/jcs.050377
3. Bloodgood RA. Chapter 1—from central to rudimentary to primary: the history of an underappreciated organelle whose time has come. The primary cilium. In: Sloboda, RD, ed. *Primary Cilia, Methods in Cell Biology*, vol 94. Academic Press; 2009:2-52. doi:10.1016/S0091-679X(08)94001-2
4. Higgins M, Obaidi I, McMorrow T. Primary cilia and their role in cancer (review). *Oncol Lett*. 2019;17:3041-3047. doi:10.3892/ol.2019.9942
5. Satir P, Christensen ST. Structure and function of mammalian cilia. *Histochem Cell Biol*. 2008;129:687-693. doi:10.1007/s00418-008
6. Huangfu D, Liu A, Rakeman AS, Murcia NS, Niswander L, Anderson KV. Hedgehog signalling in the mouse requires intraflagellar transport proteins. *Nature*. 2003;426:83-87. doi:10.1038/nature02061
7. Ezratty EJ, Stokes N, Chai S, Shah AS, Williams SE, Fuchs E. A role for the primary cilium in notch signaling and epidermal differentiation during skin development. *Cell*. 2011;145:1129-1141. doi:10.1016/j.cell.2011.05.030
8. Lancaster MA, Schroth J, Gleeson JG. Subcellular spatial regulation of canonical Wnt signalling at the primary cilium. *Nat Cell Biol*. 2011;13:700-707. doi:10.1038/ncb2259
9. Christensen ST, Clement CA, Satir P, Pedersen LB. Primary cilia and coordination of receptor tyrosine kinase (RTK) signalling. *J Pathol*. 2012;226:172-184. doi:10.1002/path.3004
10. Clement CA, Ajbro KD, Koefoed K, et al. TGF-β signaling is associated with endocytosis at the pocket region of the primary cilium. *Cell Rep*. 2013;3:1806-1814. doi:10.1016/j.celrep.2013.05.020
11. Anvarian Z, Mykytyn K, Mukhopadhyay S, Pedersen LB, Christensen ST. Cellular signalling by primary cilia in development, organ function and disease. *Nat Rev Nephrol*. 2019;15:199-219. doi:10.1038/s41581-019
12. Oh EC, Vasanth S, Katsanis N. Metabolic regulation and energy homeostasis through the primary cilium. *Cell Metab*. 2015;21:21-31. doi:10.1016/j.cmet.2014.11.019
13. Rangel L, Bernabé-Rubio M, Fernández-Barrera J, et al. Caveolin-1 αregulates primary cilium length by controlling RhoA GTPase activity. *Sci Rep*. 2019;9:1116. doi:10.1038/s41598-018
14. Kunova Bosakova M, Nita A, Gregor T, et al. Fibroblast growth factor receptor influences primary cilium length through an interaction with intestinal cell kinase. *Proc Natl Acad Sci USA*. 2019;116:4316-4325. doi:10.1073/pnas.1800338116
15. Resnick A, Hopfer U. Force-response considerations in ciliary mechanosensation. *Biophys J*. 2007;93:1380-1390. doi:10.1529/biophysj.107.105007
16. Pan J, Snell WJ. Organelle size: a cilium length signal regulates IFT cargo loading. *Curr Biol*. 2014;24:R75-R78. doi:10.1016/j.cub.2013.11.043
17. Thompson C, Plant J, Wann A, et al. Chondrocyte expansion is associated with loss of primary cilia and disrupted hedgehog signalling. *Eur Cell Mater*. 2017;34:1281-1214. doi:10.22203/eCM.v034a09
18. Wu H, Wang Z, Liu S, et al. Sub-toxic levels of cobalt ions impair chondrocyte mechanostranduction via hdac6-dependent primary cilia shortening. *Biochem Biophys Res Commun*. 2021;544:38-43. doi:10.1016/j.bbrc.2021.01.041
19. Ávalos Y, Peña-Oyarzun D, Budini M, Morselli E, Criollo A. New roles of the primary cilium in autophagy. *Biomed Res Int*. 2017;2017:4367019-4367016. doi:10.1155/2017/4367019
20. Ruhlen R, Marberry K. The chondrocyte primary cilium. *Osteoarthritis Cartilage*. 2014;22:1071-1076. doi:10.1016/j.joca.2014.05.011
21. Thompson C, McFie M, Chapple J, Beales P, Knight MM. Polycystin-2 is required for chondrocyte mechanotransduction and traffics to the primary cilium in response to mechanical stimulation. *Int J Mol Sci*. 2021;22:4313. doi:10.3390/ijms22094313
22. Farnum CE, Wilsman NJ. Orientation of primary cilia of articular chondrocytes in three-dimensional space. *Anat Rec (Hoboken)*. 2011;294:533-549. doi:10.1002/ar.21330
23. Rich DR, Clark AL. Chondrocyte primary cilia shorten in response to osmotic challenge and are sites for endocytosis. *Osteoarthritis Cartilage*. 2012;20:923-930. doi:10.1016/j.joca.2012.04.017
24. Wann AK, Knight MM. Primary cilia elongation in response to interleukin-1 mediates the inflammatory response. *Cell Mol Life Sci*. 2012;69:2967-2977. doi:10.1007/s00018-012
25. Qiu N, Xiao Z, Cao L, et al. Disruption of Kif3a in osteoblasts results in defective bone formation and osteopenia. *J Cell Sci*. 2012;125:1945-1957. doi:10.1242/jcs.095893
26. McGlashan SR, Cluett EC, Jensen CG, Poole CA. Primary cilia in osteoarthritic chondrocytes: from chondrons to clusters. *Dev Dyn*. 2008;237:2013-2020. doi:10.1002/dvdy.21501
27. Ghossoub R, Hu Q, Failler M, et al. Septins 2, 7 and 9 and MAP4 colocalize along the axoneme in the primary cilium and control ciliary length. *J Cell Sci*. 2013;126:2583-2594. doi:10.1242/jcs.111377
28. Kim JI, Kim J, Jang HS, Noh MR, Lipschutz JH, Park KM. Reduction of oxidative stress during recovery accelerates normalization of primary cilia length that is altered after ischemic injury in murine kidneys. *Am J Physiol Renal Physiol*. 2013;304:F1283-F1294. doi:10.1152/ajprenal.00427.2012
29. Dalbay MT, Thorpe SD, Connelly JT, Chapple JP, Knight MM. Adipogenic differentiation of hMSCs is mediated by recruitment of IGF-1r onto the primary cilium associated with cilia elongation. *Stem Cells*. 2015;33:1952-1961. doi:10.1002/stem.1975
30. Forcioli-Conti N, Lacas-Gervais S, Dani C, Peraldi P. The primary cilium undergoes dynamic size modifications during adipocyte differentiation of human adipose stem cells. *Biochem Biophys Res Commun*. 2015;458:117-122. doi:10.1016/j.bbrc.2015.01.078
31. Dummer A, Poelma C, DeRuiter MC, Goumans MJ, Hierck BP. Measuring the primary cilium length: improved method for unbiased high-throughput analysis. *Cilia*. 2016;5:7. doi:10.1186/s13630-0162
32. Subramanian A, Budhiraja G, Sahu N. Chondrocyte primary cilium is mechanosensitive and responds to low-intensity-ultrasound by altering its length and orientation. *Int J Biochem Cell Biol*. 2017;91:60-64. doi:10.1016/j.biocel.2017.08.018
33. Takahashi K, Nagai T, Chiba S, Nakayama K, Mizuno K. Glucose deprivation induces primary cilium formation through mTORC1 inactivation. *J Cell Sci*. 2018;13:jcs208769. doi:10.1242/jcs.208769
34. Maharjan Y, Lee JN, Kwak S, et al. Autophagy alteration prevents primary cilium disassembly in RPE1 cells. *Biochem Biophys Res Commun*. 2018;500:242-248. doi:10.1016/j.bbrc.2018.04.051
35. Guerra J, Chiodelli P, Tobia C, Gerri C, Presta M. Long-pentraxin 3 affects primary cilium in zebrafish embryo and cancer cells via the FGF system. *Cancers (Basel)*. 2020;12:1756. doi:10.3390/cancers12071756
36. Komarynets O, Chassot A, Bernabeu E, et al. Aldosterone controls primary cilium length and cell size in renal collecting duct principal cells. *FASEB J*. 2020;34:2625-2640. doi:10.1096/fj.201901947R
37. Upadhyai P, Guleria VS, Udupa P. Characterization of primary cilia features reveal cell-type specific variability in vitro models of osteogenic and chondrogenic differentiation. *PeerJ*. 2020;8:e9799. doi:10.7717/peerj.9799
38. Li B, Yan YP, Liang C, et al. Primary cilia restrain PI3K-AKT signaling to orchestrate human decidualization. *Int J Mol Sci*. 2022;23:15573. doi:10.3390/ijms232415573

39. Scarinci N, Perez PL, Cantiello HF, Cantero MDR. Polycystin-2 (TRPP2) regulates primary cilium length in LLC-PK1 renal epithelial cells. *Front Physiol*. 2022;13:995473. doi:10.3389/fphys.2022.995473

40. Franco I, Gulluni F, Campa C, et al. PI3K class II î± controls spatially restricted endosomal PtdIns3P and Rab11 activation to promote primary cilium function. *Dev Cell*. 2014;28:647-658. doi:10.1016/j.devcel.2014.01.022

41. Montero Llopis P, Senft RA, Ross-Elliott TJ, et al. Best practices and tools for reporting reproducible fluorescence microscopy methods. *Nat Methods*. 2021;18:1463-1476. doi:10.1038/s41592-021

42. Houston WV. A compound interferometer for fine structure work. *Phys Rev*. 1927;29:478-484. doi:10.1103/PhysRev.29.478

43. Wilson T. Resolution and optical sectioning in the confocal microscope. *J Microsc*. 2011;244:113-121. doi:10.1111/j.1365-2818.2011.03549.x

44. R Core Team. *R: A Language and Environment for Statistical Computing*. Vienna: R Foundation for Statistical Computing; 2022. https://www.R-project.org/

45. Schindler D, Bensmann F, Dietze S, Krüger F. The role of software in science: a knowledge graph-based analysis of software mentions in PubMed Central. *PeerJ Comput Sci*. 2022;8:e835. doi:10.7717/peerj-cs.835

46. Lauring MC, Zhu T, Luo W, Wu W, Yu F, Toomre D. New software for automated cilia detection in cells (ACDC). *Cilia*. 2019;8:1. doi:10.1186/s13630-019

47. Hansen JN, Rassmann S, Stüven B, Jurisch-Yaksi N, Wachten D. CiliaQ: a simple, open-source software for automated quantification of ciliary morphology and fluorescence in 2D, 3D, and 4D images. *Eur Phys J E Soft Matter*. 2021;44:18. doi:10.1140/epje/s10189-021-00031-y

48. Schindelin J, Arganda-Carreras I, Frise E, et al. Fiji: an open-source platform for biological-image analysis. *Nat Methods*. 2012;9:676-682. doi:10.1038/nmeth.2019

49. Morgan M. BiocManager: access the bioconductor project package repository. R package version 1.30.16, 2022. https://CRAN.R-project.org/package=BiocManager

50. Wickham H, Hester J, Chang W, et al. Devtools: tools to make developing R packages easier. R package version 2.4.5, 2022. https://CRAN.R-project.org/package=devtools

51. Ushey K, Allaire J, Tang Y. Reticulate: interface to "Python." R package version 1.26, 2022. https://CRAN.R-project.org/package=reticulate

52. Wickham H, François R, Henry L, et al. Dplyr: a grammar of data manipulation. R package version 1.0.10, 2022. https://CRAN.R-project.org/package=dplyr

53. Pau G, Fuchs F, Sklyar O, et al. EBImage—an R package for image processing with applications to cellular phenotypes. *Bioinformatics*. 2010;26:979-981. doi:10.1093/bioinformatics/btq046

54. Budde-Sagert K. readCzi: R package to read CZI image files, convert them to tifs, and save metadata. R package version 0.4.1, 2024. doi:10.5281/zenodo.10867994

55. Gohlke C. czifile: Read Carl Zeiss(r) Image (CZI) files. Python library version 2019.7.2, 2019. https://pypi.org/project/czifile/

56. Saggese T, Young AA, Huang C, Braeckmans K, McGlashan SR. Development of a method for the measurement of primary cilia length in 3D. *Cilia*. 2012;1:11. doi:10.1186/2046-2530

57. Nyquist H. Certain topics in telegraph transmission theory. *Trans Am Inst Electr Eng*. 1928;47:617-644. doi:10.1109/T-AIEE.1928.5055024

58. Shannon CE. Communication in the presence of noise. *Proc IRE*. 1949;37:10-21. doi:10.1109/JRPROC.1949.232969

59. Pawley JB. Fundamental limits in confocal microscopy. In: Pawley, J, ed. *Handbook of Biological Confocal Microscopy*, chap 2. Springer; 2006:20-42. doi:10.1007/978-0-387-45524-2_2

60. Benya PD, Shaffer JD. Dedifferentiated chondrocytes reexpress the differentiated collagen phenotype when cultured in agarose gels. *Cell*. 1982;30:215-224. doi:10.1016/0092-8674(82)90027-7

61. Lin Z, Fitzgerald JB, Xu J, et al. Gene expression profiles of human chondrocytes during passaged monolayer cultivation. *J Orthop Res*. 2008;26:1230-1237. doi:10.1002/jor.20523

62. Jonitz A, Lochner K, Peters K, et al. Differentiation capacity of human chondrocytes embedded in alginate matrix. *Connect Tissue Res*. 2011;52:503-511. doi:10.3109/03008207.2011.593673

63. Tuan RS, Chen AF, Klatt BA. Cartilage regeneration. *J Am Acad Orthop Surg*. 2013;21:303-311. doi:10.5435/JAAOS-21-05-303

64. Hu X, Zhang W, Li X, et al. Strategies to modulate the redifferentiation of chondrocytes. *Front Bioeng Biotechnol*. 2021;9:764193. doi:10.3389/fbioe.2021.764193

65. Witt A, Salamon A, Boy D, et al. Gene expression analysis of growth factor receptors in human chondrocytes in monolayer and 3D pellet cultures. *Int J Mol Med*. 2017;40:10-20. doi:10.3892/ijmm.2017.2994

66. Jonitz-Heincke A, Klinder A, Boy D, et al. In vitro analysis of the differentiation capacity of postmortally isolated human chondrocytes influenced by different growth factors and oxygen levels. *Cartilage*. 2019;10:111-119. doi:10.1177/1947603517719318

67. Ehnert S, Sreekumar V, Aspera-Werz RH, et al. TGF-1 impairs mechanosensation of human osteoblasts via HDAC6-mediated shortening and distortion of primary cilia. *J Mol Med*. 2017;95:653-663.

68. van der Valk J, Brunner D, De Smet K, et al. Optimization of chemically defined cell culture media—replacing fetal bovine serum in mammalian in vitro methods. *Toxicol In Vitro*. 2010;24:1053-1063. doi:10.1016/j.tiv.2010.03.016

69. Budde-Sagert K, Krueger S, Sehlke C, et al. Confocal microscopy images (CZI files) of human chondrocytes in different cell culture media with stained nuclei and primary cilia. *Zenodo;* 2024. doi:10.5281/zenodo.10927762

70. Budde-Sagert K, Krueger S, Sehlke C, et al. Confocal microscopy images (CZI files) of human chondrocytes in different cell culture media with stained nuclei and primary cilia. *Zenodo;* 2023. doi:10.5281/zenodo.7994589

71. Budde-Sagert K, Krueger S, Sehlke C, et al. Confocal microscopy images (CZI files) of human chondrocytes of different resolutions and magnifications with stained nuclei and primary cilia. *Zenodo;* 2023. doi:10.5281/zenodo.8038571

72. Hothorn T, Hornik K, van de Wiel MA, Zeileis A. Implementing a class of permutation tests: the coin package. *J Stat Softw*. 2008;28:1-23. doi:10.18637/jss.v028.i08

73. Johnson P. DevEMF: EMF graphics output device. R package version 4.1-2, 2022. https://CRAN.R-project.org/package=devEMF

74. Millard SP. *EnvStats: An R Package for Environmental Statistics*. Springer; 2013. doi:10.1007/978-1-4614-8456-1.

75. Clarke E, Sherrill-Mix S, Dawson C. ggbeeswarm: categorical scatter (violin point) plots. R package version 0.7.1, 2022. https://CRAN.R-project.org/package=ggbeeswarm

76. Kassambara A. ggpubr: "ggplot2" based publication ready plots. R package version 0.5.0, 2022. https://CRAN.R-project.org/package=ggpubr

77. Mount J. Rquery: relational query generator for data manipulation at scale. R package version 1.4.9, 2022. https://CRAN.R-project.org/package=rquery

78. Kassambara A. rstatix: pipe-friendly framework for basic statistical tests. R package version 0.7.1, 2022. https://CRAN.R-project.org/package=rstatix

79. Wickham H, Seidel D. Scales: scale functions for visualization. R package version 1.2.1, 2022. https://CRAN.R-project.org/package=scales

80. Wickham H, Averick M, Bryan J, et al. Welcome to the tidyverse. *J Open Source Softw*. 2019;4:1686. doi:10.21105/joss.01686